ELSEVIER

Journal of Nuclear Materials 289 (2001) 96–101

journal of nuclear materials

www.elsevier.nl/locate/jnucmat

# Accumulation and recovery of disorder on silicon and carbon sublattices in ion-irradiated 6H–SiC

W. Jiang *, W.J. Weber, S. Thevuthasan, V. Shutthanandan

*Pacific Northwest National Laboratory, P.O. Box 999 MS K8-93, 902 Battelle Boulevard, Richland, WA 99352, USA*

**Abstract**

Irradiation experiments have been performed at 100, 170 and 300 K for 6H–SiC single crystals using $Au^{2+}$ and $He^{+}$ ions over a range of fluences. The evolution of disorder on both the Si and C sublattices has been simultaneously investigated using 0.94 MeV $D^{+}$ Rutherford backscattering spectrometry (RBS) in combination with $^{12}C(d,p)$ nuclear reaction analysis (NRA) in a $\langle 0\,0\,0\,1 \rangle$ axial channeling geometry. At low doses, a higher rate of C disordering is observed, which is consistent with molecular dynamics simulations that suggest a smaller threshold displacement energy on the C sublattice. At higher doses for $He^{+}$ irradiation, the C disordering appears to increase less rapidly than the Si disordering. Three distinct recovery stages are observed on both the Si and C sublattices in the $Au^{2+}$-irradiated 6H–SiC. However, complete recovery of irradiation-induced disorder does not occur during isochronal annealing at temperatures up to 970 K. © 2001 Elsevier Science B.V. All rights reserved.

*PACS:* 61.80.Jh; 61.72.Cc; 61.82.Fk; 61.85.+p

## 1. Introduction

Irradiation-induced disordering and amorphization in several silicon carbide (SiC) polytypes have been the subject of numerous studies in recent years [1–6]. Because of its outstanding physical and nuclear properties, SiC is a promising candidate material for advanced electronic devices and a variety of nuclear applications. The potential nuclear applications for SiC include structural components in fusion reactors [7], cladding material for gas-cooled fission reactors [8] and an inert matrix for the transmutation of plutonium and other transuranics [9]. A fundamental understanding of the accumulation and recovery of irradiation-induced damage in SiC is needed to advance these technological applications. Recent scientific efforts have substantially improved the understanding of radiation damage processes in SiC and have resulted in several comprehensive reviews of the experimental investigations [1–4] and relevant theoretical models [10].

Previous studies have primarily used electrons or light to medium–heavy ions as irradiation particles, and ion mass effects on the disordering rate have been observed [2,11–13]. Although the damage energy for full amorphization at 77 K in Au-irradiated SiC has been reported [14], the temperature dependence of damage accumulation and the details of thermal recovery processes in SiC irradiated with very-heavy ions, such as Au, have not yet been reported in the literature. Previous studies of irradiation-induced defects in SiC have focused primarily on the accumulation of disorder on the Si sublattice using conventional ion-channeling methods. Electron microscopy has also been used to some extent to characterize the nature of the irradiation-induced microstructure [1,15]. The simultaneous analysis of disorder on both the Si and C sublattices has been reported previously only for $H^{+}$- and $He^{+}$-irradiated SiC [16,17] using the combination of Rutherford backscattering spectrometry (RBS) and nuclear reaction analysis (NRA) in channeling geometry. In the present paper, the accumulation and recovery of disorder on both sublattices in 6H–SiC irradiated with $Au^{2+}$ and $He^{+}$ ions are investigated based on $D^{+}$ RBS and NRA methods in channeling geometry.

* Corresponding author. Tel.: +1-509 376 5471; fax: +1-509 376 5106.

*E-mail address:* weilin.jiang@pnl.gov (W. Jiang).

0022-3115/01/$ - see front matter © 2001 Elsevier Science B.V. All rights reserved.
PII: S 0 0 2 2 - 3 1 1 5 ( 0 0 ) 0 0 6 8 7 - 5

## 2. Experimental procedures

Irradiation experiments on the ⟨0 0 0 1⟩-oriented 6H–SiC single crystals with $Au^{2+}$ and $He^{+}$ ions have been performed at the Pacific Northwest National Laboratory (PNNL) and the Research Center Rossendorf in Germany, respectively. The irradiation experiments with 2.0 MeV $Au^{2+}$ were performed over an ion fluence range from 0.02 to 0.8 ions/nm$^2$ at temperatures of 170 and 300 K. A large tilt angle (60° off surface normal) was chosen in order to produce shallow damage that could be readily measured by ion-channeling methods. The low energy (50 keV) $He^{+}$ irradiation was conducted close to the surface normal and over ion fluences ranging from 7.5 to 200 ions/nm$^2$ at 100 and 300 K. The $He^{+}$-irradiated samples were stored at room temperature for ~3 months prior to analysis. Some recovery of the accumulated disorder in the samples irradiated at 100 K was expected during the storage period [18].

Both in situ and ex situ analyses of disorder in the $Au^{2+}$- and $He^{+}$-irradiated specimens, respectively, have been carried out using the 3.4 MV tandem accelerator facility within the Environmental Molecular Sciences Laboratory at the PNNL. Simultaneous determination of disorder on both the Si and C sublattices has been achieved based on the channeling geometry for $^{28}$Si(d,d)$^{28}$Si RBS and $^{12}$C(d,p)$^{13}$C NRA at a scattering or reaction angle of 150°. A low $D^{+}$ ion energy (0.94 MeV) was selected [17] to improve the depth resolution for profiling the narrow disorder distributions in the irradiated specimens. For the $Au^{2+}$ irradiation study at 170 K, the SiC samples were maintained at this low temperature during the interim technical procedure for switching from the $Au^{2+}$ to the $D^{+}$ beam, and the RBS/NRA channeling spectra were measured in situ at or below this temperature to minimize thermal recovery of disorder in the samples. In situ isochronal annealing for 20 min was used to follow the damage recovery processes at temperatures ranging from 300 to 870 K for the SiC irradiated at 170 K with $Au^{2+}$ and from 370 to 1070 K for the SiC irradiated with $He^{+}$ at 100 K. In situ RBS/NRA analysis was performed at room temperature for all the annealed samples. An experimental error on the order of 5–10% is expected for the analysis of lattice disorder in this study. Further details about the experimental conditions and procedures have been described elsewhere [17,19,20].

For the convenience of comparing irradiation results from different ion species, the ion fluence has been converted to an equivalent dose, $D$, in units of displacements per atom (dpa) at the damage peak that is given by the expression

$$D\ (\text{dpa}) = [\Phi\ (\text{ion/cm}^2) \times R\ (\text{displacements/ion/cm})]/N\ (\text{atom/cm}^3), \quad (1)$$

where $\Phi$ is the ion fluence, $R$ the local production of displaced atoms per ion (i.e., at the damage peak), and $N$ is the atomic density of SiC. The value of $R$ is the total number of displaced atoms on both the Si and C sublattices, which has been calculated for each ion species using the SRIM-97 [21] full damage cascade simulations under the assumptions of a sample density of 3.21 g/cm$^3$ and threshold displacement energies of 20 and 35 eV for the C and Si sublattices, respectively [22,23]. At the damage peak, the conversion factor, $R/N$, from fluence in ions/nm$^2$ to dpa is 0.004296 and 0.5915 for $He^{+}$ and $Au^{2+}$, respectively, under the irradiation conditions.

## 3. Results and discussion

### 3.1. Disorder accumulation

A series of in situ 0.94 MeV $D^{+}$ RBS and NRA channeling spectra for 6H–SiC irradiated with 2.0 MeV $Au^{2+}$ at 170 K to various ion fluences are shown in Fig. 1. Also included in the figure are random-equivalent and ⟨0 0 0 1⟩-aligned spectra from a virgin area, which define the upper and lower level limits of the backscattering yields from the amorphous and essentially defect-free SiC materials, respectively. From Fig. 1, the Si damage peaks for the irradiated specimens are readily measurable from the $D^{+}$ RBS/channeling. Although the C damage peaks also appear in the RBS/channeling spectra, accurate analysis of disorder on the C sublattice is not straightforward because of the spectrum overlap. The $D^{+}$ scattering yield from the Au implants is not observable due to the very low Au concentrations. The break in the abscissa between channel numbers 200 and

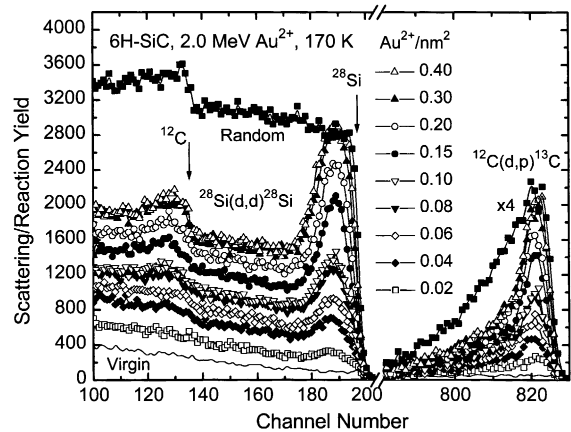


Fig. 1. A sequence of in situ 0.94 MeV $D^{+}$ RBS and NRA channeling spectra for ⟨0 0 0 1⟩-oriented 6H–SiC wafers irradiated 60° off surface normal at 170 K with 2.0 MeV $Au^{2+}$ ions. Also included are random-equivalent and channeling spectra from a virgin area.

780 contains negligible counts. From Fig. 1, the $^{12}C(d,p)^{13}C$ NRA/channeling spectra for the C disorder profiles are well resolvable in a background-free region. This condition allows simultaneous analysis of disorder on both the Si and C sublattices from one measurement.

The accumulated disorder at the damage peak for both the Si and C sublattices is shown in Fig. 2 as a function of dose (dpa) for 6H–SiC irradiated at 170 K with $Au^{2+}$ ions. Also included in the figure are the data previously reported [17] for 6H–SiC irradiated at 100 K with 50 keV $He^{+}$ ions and stored at 300 K for ~3 months prior to analysis. Complete amorphization on both the Si and C sublattices corresponds to a relative disorder of 1.0. The solid lines in Fig. 2 are data fits using the direct-impact/defect-stimulated (DI/DS) model for amorphization that has been described previously [10] and is given by the expression

$$f_a = 1 - (\sigma_a + \sigma_s)/\{\sigma_s + \sigma_a \exp[(\sigma_a + \sigma_s)D]\}, \quad (2)$$

where $f_a$ is the amorphous fraction, $\sigma_a$ the amorphization cross-section, $\sigma_s$ the effective cross-section for DS amorphization, and $D$ is the dose. This sigmoidal-like dependence of relative disorder on dose has also been observed previously for 6H–SiC irradiated with other ion species at or below room temperature [11–13,19,24] and the 50 keV $He^{+}$ results are consistent with a previous study of $He^{+}$-irradiated SiC [18].

From Fig. 2, the 6H–SiC becomes fully amorphous at ~0.85 dpa under $He^{+}$ irradiation at 100 K and at ~0.24 dpa under $Au^{2+}$ irradiation at 170 K, which indicates an increasing rate of disordering with increasing ion mass. This higher disordering rate for $Au^{2+}$ is consistent with a higher probability for DI amorphization, within the context of the model, and with recent MD simulations [25,26] that indicate that amorphization occurs directly within large clusters produced by Au ions in SiC. For both the $Au^{2+}$ and $He^{+}$ irradiations, the data in Fig. 2 indicate that the C disorder is slightly higher at the lowest doses. This behavior, which is discussed further below, is consistent with a smaller threshold displacement energy on the C sublattice, as reported for molecular dynamics simulations [22,23,27] and other experimental measurements [16,28]. At higher doses for the $He^{+}$ irradiation, the residual disorder on the Si sublattice appears to be in excess of that on the C sublattice. Since the sample was stored at room temperature for an extended time and defect recovery is expected during the storage period, the result may suggest that at higher doses a slightly higher dynamic/thermal recovery rate may be occurring on the C sublattice than on the Si sublattice. This could also reflect some effect from the trapping of the implanted helium atoms at defects in the $He^{+}$-irradiated 6H–SiC.

Irradiation with $Au^{2+}$ and $He^{+}$ at room temperature (300 K) results in a similar sigmoidal dependence of disorder on dose, as shown in Fig. 3. The results in Fig. 3 indicate that the rate of disordering has decreased with the increase in irradiation temperature for both the $Au^{2+}$ and $He^{+}$ in agreement with the kinetic form of the DI/DS model [10] that accounts for the dynamic recovery processes. From Fig. 3, the dose to achieve the fully amorphous state increases at 300 K to ~0.35 dpa and >1.1 dpa for the $Au^{2+}$ and $He^{+}$, respectively. This decrease in disordering rate is primarily attributed to a higher dynamic recovery rate at the higher irradiation

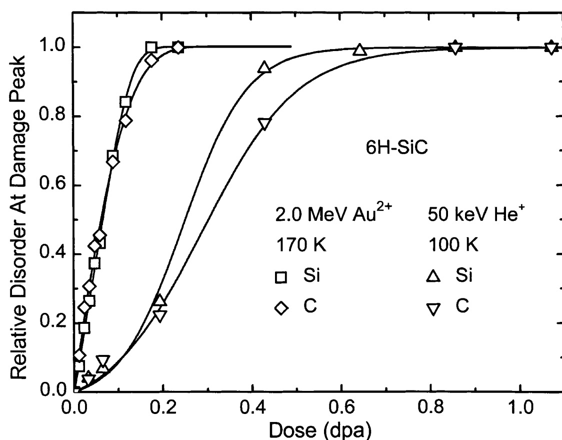


Fig. 2. Relative disorder on the Si and C sublattices as a function of dose (dpa) at the damage peak for 2.0 MeV $Au^{2+}$-irradiated 6H–SiC at 170 K. Also included are the results for the 6H–SiC irradiated at 100 K with 50 keV $He^{+}$ ions and stored at 300 K for ~3 months prior to analysis. Solid lines are the data fits using the DI/DS model (Eq. (2)).

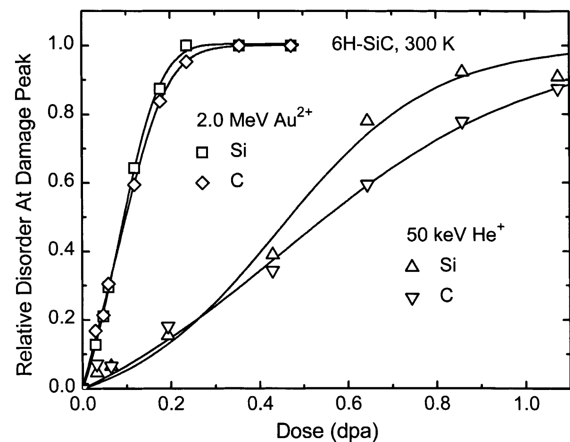


Fig. 3. Relative disorder on the Si and C sublattices as a function of dose (dpa) at the damage peak for 2.0 MeV $Au^{2+}$-irradiated 6H–SiC at 300 K. Also included are the results for the 6H–SiC irradiated at 300 K with 50 keV $He^{+}$ ions. Solid lines are the data fits using the DI/DS model (Eq. (2)).

temperature (300 K). As with the irradiation at low temperatures, the results in Fig. 3 show a strong dependence on ion mass.

In order to examine the ratio of C-to-Si disorder as a function of dose, two curves under the low temperature irradiation conditions (Fig. 2) are plotted in Fig. 4. At low doses, the ratio tends to increase with the decrease of dose. The extrapolation to zero dose results in a ratio of about 2 for $He^+$ irradiation at 100 K. This result is consistent with the MD simulations [26,27,29] that give a value between 2 and 3 for a single cascade. As discussed above, the higher degree of C disorder may be associated with the smaller displacement energy on the C sublattice. The different ratios at low doses under the $Au^{2+}$ irradiation conditions may be partly attributed to the formation of large Si and C clusters and localized amorphous zones that are produced directly in the cascades [25,26]. The production of clusters or amorphous domains may be less dependent on the different displacement energies for Si and C sublattices as compared to the formation single atomic displacements (i.e., Frenkel pairs).

The ratio of C-to-Si disorder (Fig. 4) decreases with increasing dose and becomes less than 1.0 at intermediate doses. For the $Au^{2+}$-irradiation data, this decrease in the ratio below 1.0 is within the experimental uncertainty. However, for the $He^+$-irradiation data, the results clearly show that the Si disorder exceeds the C disorder at intermediate damage levels. The excess of the Si disorder under $He^+$ irradiation suggests that a higher rate of recovery may be occurring on the C sublattice relative to the Si sublattice. Additionally, the trapping of implanted helium atoms may be affecting the relative recovery rates. For both $Au^{2+}$ and $He^+$ irradiations, the dose for full amorphization on both sublattices occurs at the same dose and the ratio becomes equal to 1.0 (the dotted-line level). The results in Fig. 4 provide further evidence of the effects of ion mass on amorphization behavior.

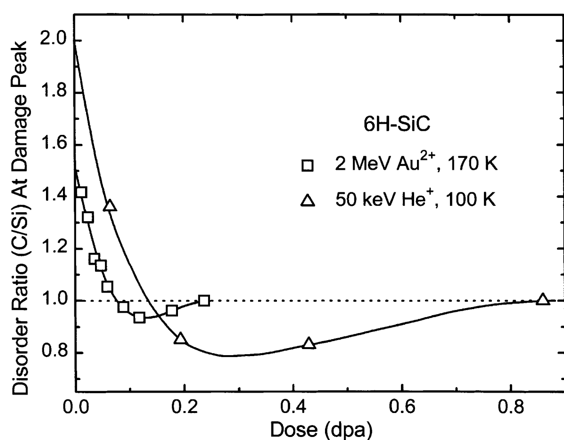


Fig. 4. Ratio of disorder on the C-to-Si sublattice, derived from the experimental data in Fig. 2, as a function of dose (dpa).

### 3.2. Disorder recovery

A sequence of RBS and NRA channeling spectra is shown in Fig. 5 for SiC irradiated at 300 K to an ion fluence of 0.2 $Au^{2+}/nm^2$ and subsequently annealed at 420, 570, 720 and 870 K for 20 min each. From the results in Fig. 5, a clear recovery stage on both Si and C sublattices is observed between 420 and 570 K. This recovery stage was suggested in the results of a recent study of $C^+$-irradiated 6H–SiC [30] under similar annealing conditions. The recovery behavior (Stage B) is also observed for the SiC irradiated at 170 K to 0.15 $Au^{2+}/nm^2$ and isochronally annealed under similar conditions at successively higher temperatures, as shown in Fig. 6. The data in Fig. 6 also suggest that additional recovery stages (Stages A and C) occur between 170 and 300 and above 570 K, respectively, which are consistent with previous observations [30].

The results from the isochronal annealing of SiC irradiated at 170 K with $Au^{2+}$ to various ion fluences are shown in Fig. 7 and exhibit similar recovery behavior on the Si and C sublattices. Significant recovery processes on both sublattices occur below room temperature (Stage A), between 420 and 570 K (Stage B), and above 570 K (Stage C). The activation energies for the recovery processes associated with Stages A and C on the Si sublattice have been recently estimated to be of the order of $0.25 \pm 0.15$ and $1.5 \pm 0.3$ eV, respectively, using a

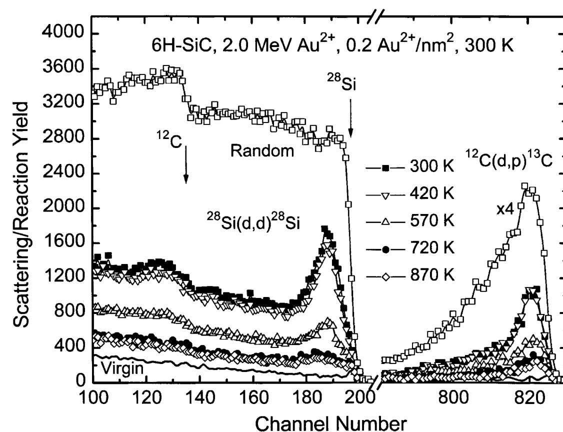


Fig. 5. A sequence of in situ 0.94 MeV $D^+$ RBS and NRA channeling spectra for ⟨0 0 0 1⟩-oriented 6H–SiC wafers irradiated 60° off surface normal at 300 K to an ion fluence of 0.2 $Au^{2+}/nm^2$ and annealed at successively higher temperatures for 20 min each. Also included are random-equivalent and channeling spectra from a virgin area.

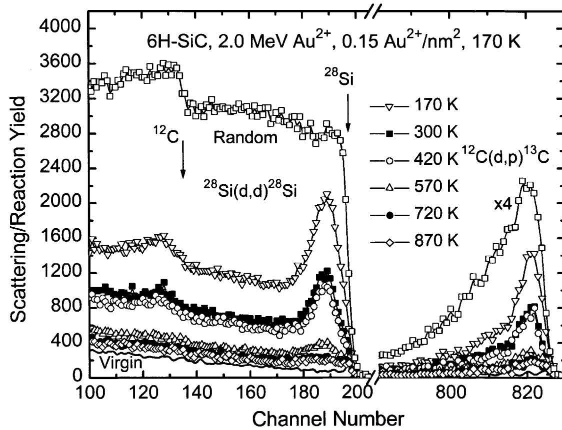


Fig. 6. A sequence of in situ 0.94 MeV $D^+$ RBS and NRA channeling spectra for ⟨0 0 0 1⟩-oriented 6H–SiC wafers irradiated 60° off surface normal at 170 K to an ion fluence of 0.15 $Au^{2+}/nm^2$ and annealed at successively higher temperatures for 20 min each. Also included are random-equivalent and channeling spectra from a virgin area.

combination of isothermal and isochronal annealing results [30]. A more recent evaluation gives an uncertainty of ±0.15 eV for the Stage A recovery rather than the ±0.1 eV that was reported [30]. Additional experiments are planned to determine the activation energies for all the observed recovery stages on the Si and C sublattices. Since ion-channeling method does not generally identify the defect types responsible for the recovery stages, computer simulations will be necessary to identify the detailed underlying processes.

While there is a rapid recovery of disorder below room temperature for the lowest dose sample in Fig. 7, complete recovery is not observed at higher temperatures. Instead, there is a gradual recovery of this residual level of disorder (~0.1) with increasing anneal temperature over a wide range of temperatures. Complete recovery of this residual disorder is not observed on either the Si or C sublattices for anneals up to 870 K. This result is in contrast with that for $Si^+$-irradiated 6H–SiC [19], where a complete recovery of disorder is observed below room temperature for a comparable level of disorder. The difference is attributed to the higher probability of cluster formation and in-cascade amorphization for $Au^{2+}$ ions compared to $Si^+$ ions [25,26], which are more thermally stable than isolated point defects. The annihilation of irradiation-induced point defects below room temperature is expected to result in some annealing of such amorphous domains and clusters. However, any remaining clusters and amorphous domains are expected to be relatively stable up to ~1300 K where recrystallization is first observed to occur [15], or up to ~1450 K where very rapid recrystallization proceeds [3,15].

A similar thermal recovery behavior is observed for the $He^+$-irradiated SiC, as shown in Fig. 8. The isochronal annealing (20 min) was performed on the SiC irradiated at 100 K after storage at room temperature for ~3 months. Based on previous results for $He^+$-irradiated SiC [18], some defect recovery was expected for the low to intermediate damage levels during the storage period. The results in Fig. 8 show that significant defect recovery occurs at relative disorder levels from 0.2 to 0.8 on both Si and C sublattices between 350 and 1000 K. At low damage levels (below relative disorder of 0.1), the recovery rate on both sublattices is relatively slow, which indicates that all mobile defects have already recovered and any residual defects may be immobile due to He trapping [17]. Distinct recovery stages are not as apparent in these samples, which might again be associated with the He trapping at defects that inhibits defect migration and recombination for some types of defects

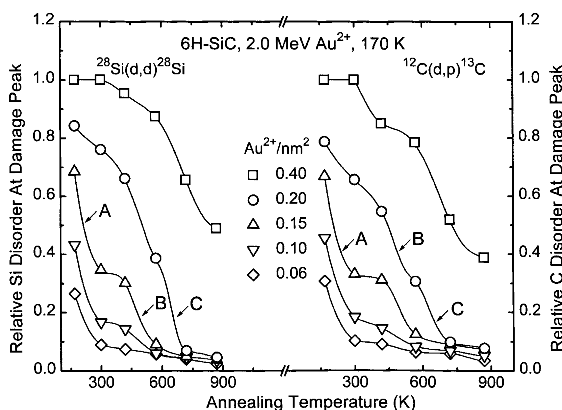


Fig. 7. Isochronal recovery (20 min) of relative disorder on the Si and C sublattices in $Au^{2+}$-irradiated 6H–SiC as a function of annealing temperature.

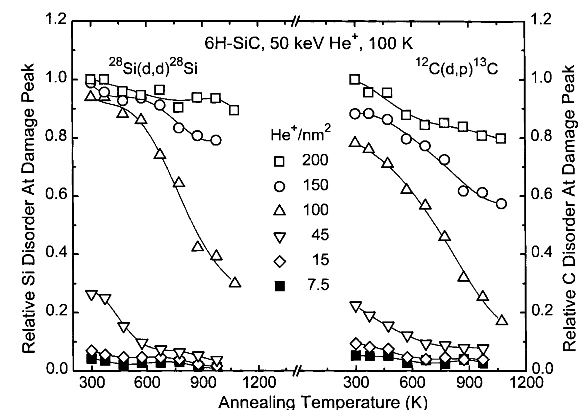


Fig. 8. Isochronal recovery (20 min) of relative disorder on the Si and C sublattices in $He^+$-irradiated 6H–SiC as a function of annealing temperature.

associated with the recovery stages observed for the $Au^{2+}$-irradiated specimens. Similar in situ recovery results for $He^{+}$-irradiated 6H–SiC at 190 K have also been reported in a separate study [18].

## 4. Summary

At each irradiation temperature (100, 170, and 300 K), the damage accumulation on both the Si and C sublattices in 6H–SiC irradiated with $Au^{2+}$ and $He^{+}$ ions shows sigmoidal-like dependence of relative disorder on dose. The rate of disordering on both Si and C sublattices decreases with decreasing ion mass and increasing irradiation temperature. A higher disordering rate is observed on the C sublattice relative to the Si sublattice at low doses (defect concentrations), which is consistent with a smaller threshold displacement energy on the C sublattice. In the case of $He^{+}$ irradiation, the residual disorder on the Si sublattice is in excess of that on the C sublattice at intermediate doses (damage levels) prior to full amorphization. For $Au^{2+}$ irradiation, three distinct defect recovery stages are observed on both sublattices under isochronal annealing (20 min) conditions. These recovery stages occur below 300 K, between 420 and 570 K, and above 570 K. For $Au^{2+}$ irradiation at 170 K, the residual low level disorder (<0.1) after annealing is attributed to in-cascade defect clusters and amorphous domains that are thermally stable to high temperatures.

## Acknowledgements

This study was supported by the Division of Materials Sciences, Office of Basic Energy Sciences, US Department of Energy. Support for the accelerator facilities within the Environmental Molecular Sciences Laboratory (EMSL) was provided by the Office of Biological and Environmental Research, US Department of Energy. The Pacific Northwest National Laboratory is operated by Battelle Memorial Institute for the US Department of Energy under Contract DE-AC 06-76RLO 1830.

## References

[1] S.J. Zinkle, L.L. Snead, Nucl. Instrum. and Meth. B 116 (1996) 92.
[2] W.J. Weber, L.M. Wang, N. Yu, N.J. Hess, Mater. Sci. Eng. A 253 (1998) 62.
[3] C.J. McHargue, J.M. Williams, Nucl. Instrum. and Meth. B 80&81 (1993) 889.
[4] E. Wendler, A. Heft, W. Wesch, Nucl. Instrum. and Meth. B 141 (1998) 105.
[5] W. Bolse, Nucl. Instrum. and Meth. B 141 (1998) 133.
[6] V. Heera, J. Stoemenos, R. Kögler, W. Skorupa, J. Appl. Phys. 77 (1995) 2999.
[7] P. Fenici, A.J.F. Rebelo, R.H. Jones, A. Kohyama, L.L. Snead, J. Nucl. Mater. 258 (1998) 215.
[8] J.C. Zink, Power Eng. (1998) 10.
[9] R.A. Verrall, M.D. Vlajic, V.D. Krstic, J. Nucl. Mater. 274 (1999) 54.
[10] W.J. Weber, Nucl. Instrum. and Meth. B 166&167 (2000) 98.
[11] W.J. Weber, N. Yu, L.M. Wang, J. Nucl. Mater. 253 (1998) 53.
[12] W.J. Weber, W. Jiang, S. Thevuthasan, D.E. McCready, Mater. Res. Soc. Symp. Proc. 540 (1999) 159.
[13] W. Jiang, W.J. Weber, S. Thevuthasan, D.E. McCready, Nucl. Instrum. and Meth. B 148 (1999) 557.
[14] W. Bolse, J. Conrad, F. Harbsmeier, M. Borowski, T. Rödle, Mater. Sci. Forum 248&249 (1997) 319.
[15] L.L. Snead, S.J. Zinkle, J.C. Hay, M.C. Osborne, Nucl. Instrum. and Meth. B 141 (1998) 123.
[16] I. Nashiyama, T. Nishijima, E. Sakuma, S. Yoshida, Nucl. Instrum. and Meth. B 33 (1988) 599.
[17] W. Jiang, S. Thevuthasan, W.J. Weber, R. Grötzschel, Nucl. Instrum. and Meth. B 161–163 (2000) 501.
[18] W. Jiang, W.J. Weber, S. Thevuthasan, D.E. McCready, J. Nucl. Mater. 257 (1998) 295.
[19] W. Jiang, W.J. Weber, S. Thevuthasan, D.E. McCready, Nucl. Instrum. and Meth. B 143 (1998) 333.
[20] W. Jiang, W.J. Weber, S. Thevuthasan, J. Appl. Phys. 87 (2000) 7671.
[21] J.F. Ziegler, J.P. Biearsack, U. Littmark, The Stopping and Range of Ions in Solids, Pergamon Press, New York, 1985.
[22] R. Devanathan, T. Diaz de la Rubia, W.J. Weber, J. Nucl. Mater. 253 (1998) 47.
[23] R. Devanathan, W.J. Weber, J. Nucl. Mater. 278 (2000) 258.
[24] W. Jiang, W.J. Weber, S. Thevuthasan, D.E. McCready, Nucl. Instrum. and Meth. B 148 (1999) 562.
[25] F. Gao, W.J. Weber, W. Jiang, Phys. Rev. B (submitted).
[26] F. Gao, W.J. Weber, R. Devanathan, Nucl. Instrum. and Meth. B (in press).
[27] J.M. Perlado, L. Malerba, A. Sanchez-Rubio, T. Diaz de la Rubia, J. Nucl. Mater. 276 (2000) 235.
[28] S.J. Zinkle, C. Kinoshita, J. Nucl. Mater. 251 (1997) 200.
[29] R. Devanathan, W.J. Weber, T. Diaz de la Rubia, Nucl. Instrum. and Meth. B 141 (1998) 118.
[30] W.J. Weber, W. Jiang, S. Thevuthasan, Nucl. Instrum. and Meth. B 166&167 (2000) 410.